

Thermodynamic-Geophysical Modeling of the Interior Structure of the Siberian Cratonic Mantle along Cross-Cutting Profiles Kimberlite and Meteorite

Kuskov OL^{1*}, Kronrod VA¹ and Pavlenkova NI²

¹Vernadsky Institute of Geochemistry and Analytical Chemistry, Russian Academy of Sciences, Moscow, Russia

²Shmidt Institute of Physics of the Earth, Russian Academy of Sciences, Moscow, Russia

Abstract

Using a thermodynamic-geophysical approach, we map the 2-D interior structure of the Siberian cratonic mantle along the ultra-long cross-cutting seismic profiles Kimberlite and Meteorite carried out in Russia with peaceful nuclear explosions. There is a systematic decrease in temperature from west to east for the Kimberlite profile and a weak decrease from NW to SE for the Meteorite profile. Cratonic mantle shows a significant heterogeneity in the distribution of seismic velocities, temperature and density, topography of seismic boundaries and degree of layering at depths up to ~200 km reflecting somewhat different thermal state along both seismic profiles. Temperatures in the central part of the craton are somewhat lower than those at the periphery and 300-400°C lower than the average temperature in the surrounding mantle. A change of composition from depleted to fertile material reveals a negligible effect on seismic velocities that is practically unresolved by seismic methods, but remains the most important factor for the density increase of cratonic root. The distribution of density in the mantle cannot be attributed to any single composition, either depleted or enriched in basaltic components. This finding suggests a significant fertilization with depth and is compatible with the chemical stratification in the root of the craton. The thickness of the thermal boundary layer (TBL, conductive lid + transition layer) can be estimated as 300 ± 30 km thick along the Kimberlite and Meteorite profiles. At the base of the TBL, the temperature is close to 1450 ± 100°C isotherm; the calculated density corresponds to the PREM model density.

Keywords: Siberian craton; Seismic profiles; Thermo-chemical structure; Xenoliths; Mantle composition

Introduction

It is believed that cratons are stable domains, which experienced practically no changes in the process of subsequent tectonic evolution. Cratons are characterized by a thick and cold lithosphere composed of a highly depleted relatively low density peridotite with very high average Mg number of olivine, elevated bulk MgO contents and low bulk Al and Ca contents, which is likely isolated from the ambient mantle for billions of years [1-8]. The significant depletion of these elements with respect to fertile mantle is responsible for cratonic mantle densities being significantly lower than that of the normal convecting mantle [1,9-12]. Knowledge of the thermal regime, thickness and composition of the mantle beneath ancient cratons is important to both fundamental geochemical-geophysical research and diamond exploration. Investigations of the mantle beneath the Siberian craton (SC) have been performed in a number of thermal, seismic and tomographic studies [13-18].

Temperature of the Earth's interior remains one of the most speculative and uncertain physical parameters, and merit further investigation. Thermobarometric results for Siberian mantle xenoliths of garnet, garnet-spinel, spinel peridotites, and pyroxenites [2,3,7,8,19] provide unique information about the compositional heterogeneity and evolution of the cratonic mantle, but do not give direct information about its seismic structure. Thermal and seismic studies provide only indirect information about the composition and temperature of cratonic mantle. Combinations of surface heat flow measurements, geophysical data, xenolith thermobarometry and additional thermodynamic constraints reduce some of the ambiguity in interpretations of mantle structure and provide the tighter constraints on mantle chemistry and thermal regime.

Seismic studies are probably one of the best tools to infer the thermal state of the upper mantle because seismic velocities are more

sensitive to temperature than to composition [20]. A set of geophysical data (global *P*- and *S*-wave travel times, surface-wave phase velocities, travel time data from the deep seismic sounding) or simply seismic velocity-depth profiles can be converted to temperature-depth profiles using petrological constraints on the mantle composition or the composition of xenoliths brought to the surface and a thermodynamic-based inversion scheme [10-12,20-27].

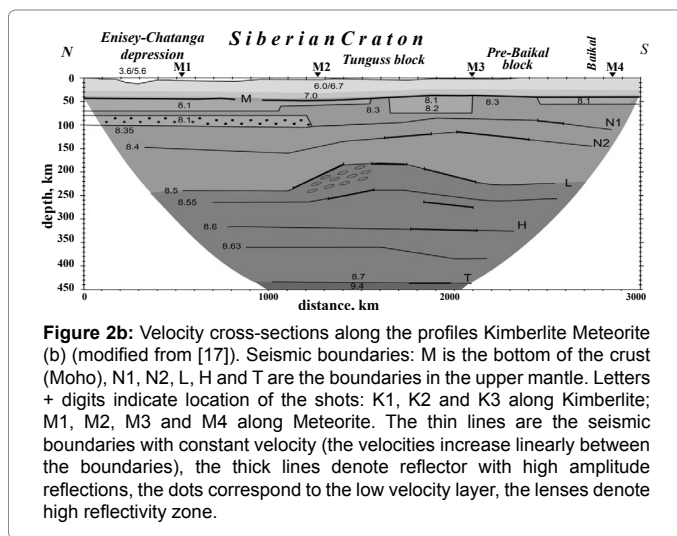
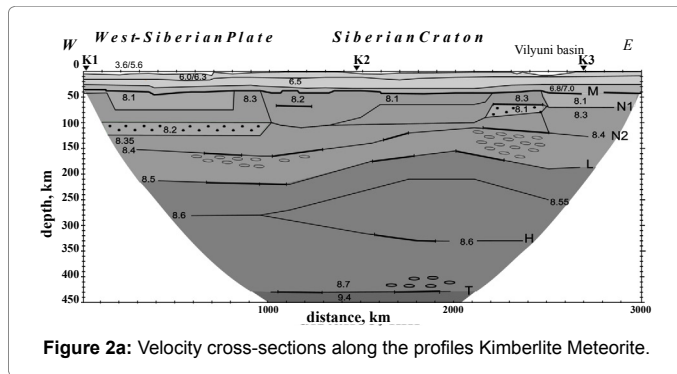
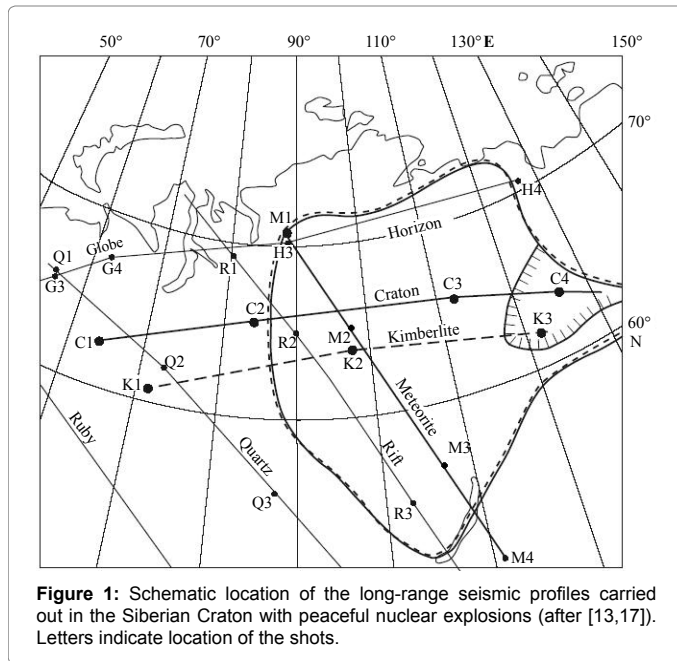
The major purpose of the present study is to estimate the thermal state, density and thickness of the lithospheric mantle beneath the Siberian craton from absolute *P*-wave velocity models along cross-cutting long-range seismic profiles (Kimberlite and Meteorite) carried out in Russia with peaceful nuclear explosions (Figure 1). The crucial question is whether the mantle material with velocities derived from seismic studies can satisfy both velocities calculated from geochemical models based on xenolith data and temperatures calculated from thermal models. For comparison of thermal regime, velocity and density of cold cratonic mantle with average upper mantle, it is instructive to use the AK135 and PREM reference models [28,29] which have formed the basis for interpreting the constitution of the Earth. It appears that the problems of assessing the thermo-chemical and thermo-physical properties (temperature, velocity, bulk moduli and density) and modeling the chemical composition are intimately

*Corresponding author: Oleg L Kuskov, Vernadsky Institute of Geochemistry and Analytical Chemistry, Russian Academy of Sciences, Kosygin Str. 19, 119991 Moscow B-334, Russia, Tel: +7(499)1378614; Fax: +7(495)9382054; E-mail: ol_kuskov@mail.ru

Received January 17, 2014; Accepted March 28, 2014; Published April 01, 2014

Citation: Kuskov OL, Kronrod VA, Pavlenkova NI (2014) Thermodynamic-Geophysical Modeling of the Interior Structure of the Siberian Cratonic Mantle along Cross-Cutting Profiles Kimberlite and Meteorite. J Geol Geosci 3: 155. doi: 10.4172/2329-6755.1000155

Copyright: © 2014 Kuskov OL, et al. This is an open-access article distributed under the terms of the Creative Commons Attribution License, which permits unrestricted use, distribution, and reproduction in any medium, provided the original author and source are credited.



density of the mantle; (2) to map the 2-D seismic, thermal and density state of the Siberian mantle; (3) to compare the inferred temperatures with heat-flow models and mantle paleotemperatures estimated from thermobarometric results; (4) to find out the effect of composition on the thickness of the thermal boundary layer; (5) to provide the better constraints on the seismic and thermo-chemical structure of the mantle in central Siberia.

Siberian Craton

Seismic velocity models

The crustal and mantle structure under the Siberian Platform was studied by the GEON Center of the USSR with chemical and peaceful nuclear explosions (PNE), Figure 1. It is the unique network of long-range profiles, where P waves from PNEs were recorded at epicentral distances reaching 3000 km. In this distance range the P waves sample the Earth from the surface to the mantle transition zone; no reliable data on the S-velocities are available. The seismic data for the profiles shown in Figure 1 were interpreted by several Russian and international groups [13,14,16,17]. These models are similar in average changes of the velocity with depth (within 0.1-0.2 km s⁻¹), although they differ in the profile cross points and contain different thin layers with higher and lower velocity. The dissimilarity between different models may be generally due to inversion methodology (Figure 1). We map the average thermal and density structure of the Siberian mantle at depths of 100 to 300 km from the seismic models presented by Pavlenkova and Pavlenkova [17] and partly modified in this study (Figure 2). The 2-D velocity models of the crust and upper mantle were constructed for the cross-cutting profiles Kimberlite and Meteorite using the both PNE and chemical explosion records. The latter gave the opportunity to correct the mantle travel times for the crustal inhomogeneity and to increase the data on the uppermost mantle structure, which was difficult to get from the PNE records alone. Before the velocity modeling the wave analysis was made for the determination of regular waves and their traveltimes changes along the profiles. The intercept-time method [30] was used for the construction of the time cross-sections and for the determination of reliable starting velocity models. The resulting velocity cross-sections along the profiles Kimberlite and Meteorite are presented in Figure 2. Their reliability was tested by their comparison in the cross-points of profiles (Figure 1); they show good agreement in the velocities at the level of 0.05 km s⁻¹ at depths between 50 and 200 km and 0.1 km s⁻¹ in the deeper part. The upper mantle is shown to be of layered structure, with reflecting boundaries at depths of about 100, 150, 240, and 320 km and velocities changing from 8.2 to 8.7 km s⁻¹. The boundaries are not simple discontinuities, but heterogeneous (thin layering) zones, which can be associated with rheological boundaries [31]. We use only average mantle velocity structure. In the central part of the SC, lateral changes in seismic velocities are observed from west to east for the Kimberlite profile (Figure 2a) and from NW to SE for the Meteorite profile (Figure 2b); no low velocity zone has been detected at depths greater than 100 km (Figures 2a and b). Figure 3 shows an example of P-velocity section from the 2-D models (Figure 2) compared with the AK135 reference model [29] and velocities calculated here for garnet peridotite xenoliths from the Devonian Udachnaya pipe [8]. The regional velocities are faster than in the standard model up to 250-300 km depth. In general, velocities for xenoliths are located between the global and regional velocities. Cross-cutting profiles Kimberlite and Meteorite suggest that the observed velocities have a significant isotropic component, since the shot points M2 and K2 situated in the neighbourhood (Figure 1) reveal similar velocities at depths of 100 to 140 km (Figure 3).

related. Solving them simultaneously will result in the construction of a self-consistent petrological-geophysical model of the deep interior. With this in mind, the main objectives of our study are as follows: (1) to determine the effect of composition and temperature on the velocity and

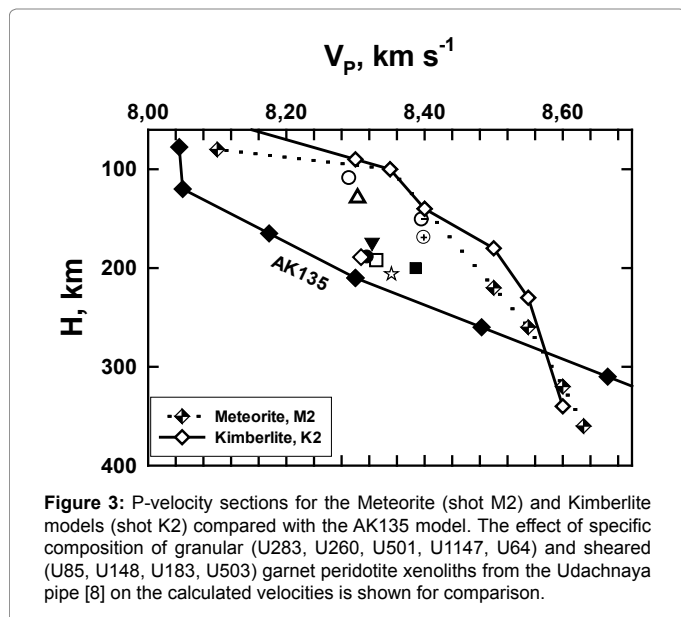


Figure 3: P-velocity sections for the Meteorite (shot M2) and Kimberlite models (shot K2) compared with the AK135 model. The effect of specific composition of granular (U283, U260, U501, U1147, U64) and sheared (U85, U148, U183, U503) garnet peridotite xenoliths from the Udachnaya pipe [8] on the calculated velocities is shown for comparison.

Composition

The composition and structure of the Siberian lithospheric mantle are constrained by a wide range of geochemical and geophysical data. According to the isotopic studies of peridotite and eclogite xenoliths and garnets in diamonds, the model age of the lithosphere is estimated to range from 2.6 to 3.2 Ga [32] that agrees with the age of the material composing the craton (the time of magma intrusion from the mantle sources to the crust) [4]. Based on seismic, thermal and thermobarometric data and physics of minerals, it is assumed that the old and cold lithosphere is depleted in basaltic components [2-8], is characterized by a low heat flow [15,18,33], low/high-velocity anomalies and lacks zones of partial melting [13,16,17]. The Siberian craton is characterized by surface heat flow averaging 38-40 mW m⁻²; in the northeastern and central areas of the craton the heat flow value is estimated as 20-30 mW m⁻² [15]. The latter indicates that the lithosphere may be up to 350 km thick [18].

Additional constraints on the thermochemical structure of the mantle are provided by xenolith data. Thermobarometric results for Siberian mantle xenoliths from kimberlites are reviewed recently [7]. Compositional spectrum of cratonic peridotites, which display a range of major element compositions as well as the thickness of thermal boundary layer vary from craton to craton, depending on their stabilization age, tectonic history and thermal regime [4-6]. The study of xenoliths in the diamond-bearing kimberlites yields unique information about the composition and structure of the mantle and indicates that a large portion of the thick cratonic lithosphere (cratonic keel) is largely composed of depleted peridotites, which is associated with the early stage of the crustal development. They consist of olivine and orthopyroxene with subordinate garnet and clinopyroxene [2,3,8,19,32]. Other lithologies that occur in the mantle are significantly less abundant than peridotites. The spinel-bearing lherzolite varieties prevail at shallower depths. According to many studies [1,2,12,19], the depletion of ultramafic rocks decreases with depth. Despite the fact that these rocks exhibit no strict succession as to the extent of their depletion, it can probably be assumed that cratonic mantle has a strongly depleted composition down to depths of 150–180 km. Beyond this depth, there appears to be a pronounced increase in fertility; i.e., the mantle material becomes gradually enriched with basaltic components (FeO, Al₂O₃,

CaO) with depth, probably up to samples from the top of the fertile convecting mantle [11,12,34,35].

Thermodynamic Approach

The thermodynamic basis for modeling phase equilibria and physical properties of the Earth's mantle and various databases have been discussed in a series of papers. We basically use the same method as that described in detail in our previous publications [11,20]. Briefly, this is a thermodynamically self-consistent approach based on a method of minimization of the Gibbs free energy in conjunction with the thermal equation of state for solids written in a Mie–Grüneisen–Debye form. The approach relates the equilibrium mineral assemblage for an assumed mantle composition and equations of state (EOS) of minerals with seismic properties. The phase composition and physical properties of the mantle were modeled within the dry Na₂O–TiO₂–CaO–FeO–MgO–Al₂O₃–SiO₂ (NaTiCFMAS) system including the non-ideal solid solution phases (Table 1). The pressure – depth correlation was

Composition	GP	PM	Hzb	Lh
SiO ₂	45.42	45.25	45.7	46.15
TiO ₂	0.08	0.21	0.02	0.05
Al ₂ O ₃	1.32	4.5	0.4	1.21
FeO	7.03	8.48	6.14	6.55
MgO	45.28	37.58	47.51	45.25
CaO	0.78	3.64	0.2	0.71
Na ₂ O	0.09	0.34	0.03	0.08
Total	100	100	100	100
MG#	92	88.8	93.2	92.5
Phase composition, physical properties 100 km (P = 2.9 GPa, 600°C)				
OI	65.8(Fe _{92.8})	55.8(Fe _{92.5})	67.3(Fe _{93.4})	61.7(Fe _{93.2})
Gar	1.5	5.4	0.37	1.3
Opx	27	10	30.9	32
Cpx	5.6	28.4	1.4	4.9
Ilm	0.1	0.4	0.03	0.1
ρ, γ χμ ⁻³	3.334	3.403	3.309	3.325
V _p , km s ⁻¹	8.32	8.332	8.323	8.314
V _s , km s ⁻¹	4.724	4.695	4.739	4.73
K _s , GPa	131.58	136.25	130.13	130.64
G, GPa	74.4	75.02	74.31	74.4

^aThe NaTiCFMAS system includes the following solid solution phases: olivine (Ol), spinel (Sp), plagioclase (Pl) and ilmenite (Ilm) – binary solutions; garnet (Gar: almandine, pyrope, grossular); orthopyroxene (Opx: MgSiO₃, FeSiO₃, Ca_{0.5}Mg_{0.5}SiO₃, Ca_{0.5}Fe_{0.5}SiO₃, Al₂O₃); clinopyroxene (Cpx: same components as in Opx plus jadeite end-member). Bulk compositions normalized to 100% were taken from Griffin et al. (2003) for Hzb and Lh (Daldyn Field, Siberia, Archon) and from McDonough (1990) for the GP and PM compositions. Total Ti is included in ilmenite. The compositions of phase assemblages (mol%) at 2.9 GPa and 600°C are given as an example.

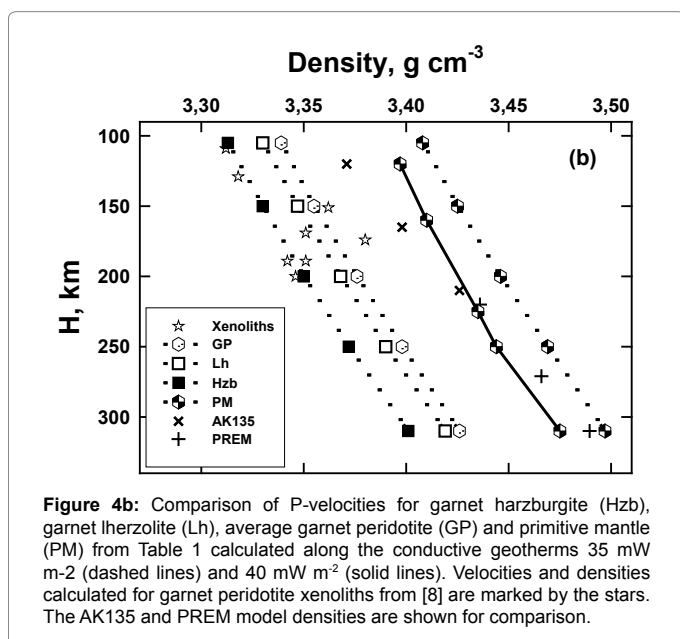
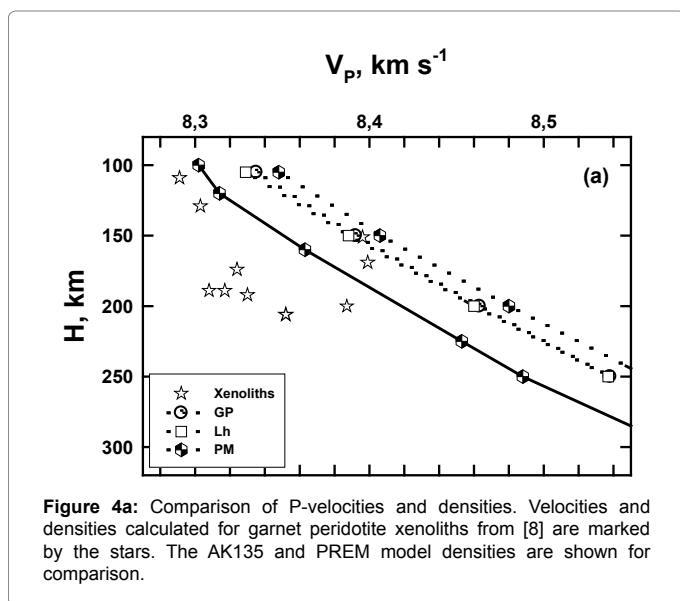
GP: 65.8% Ol (Fe_{92.8}) + 27% Opx (En_{92.2}OrthoDi_{0.4}OFS_{0.2}OrthoCor_{0.2}) + 1.5% Gar (Py₇₀Alm₂₄Gros₆) + 5.6% Cpx (ClEn₂₄Di₄₂ClFS_{6.2}Hed_{13.2}Jd₁₄ClCor_{0.8}).

PM: 55.8% Ol (Fe_{92.5}) + 5.4% Gar (Py₈₆Alm₂₅Gros₇) + 10% Opx (En₉₂OrthoDi_{0.4}OrthoFS_{0.2}OrthoHed_{0.2}OrthoCor_{0.2}) + 28.4% Cpx (ClEn_{38.7}Di_{31.8}ClFS₆Hed_{14.8}Jd_{8.5}ClCor_{0.2}).

Hzb: 67.3% Ol (Fe_{93.3}) + 0.4% Gar (Py₇₄Alm₂₃Gros₄) + 1.4% Cpx (ClEn₂₅Di_{37.8}ClFS₅Hed_{12.4}Jd₁₈ClCor_{0.8}) + 30.9% Opx (En_{92.8}OrthoDi_{0.3}OrthoFS_{0.5}OrthoHed_{0.2}OrthoCor_{0.2}).

Lh: 61.7% Ol (Fe₉₃) + 1.3% Gar (Py₇₁Alm₂₃Gros₆) + 32% Opx (En_{92.5}OrthoDi_{0.4}OrthoFS_{0.7}OrthoHed_{0.2}OrthoCor_{0.2}) + 5% Cpx (ClEn₂₄Di₄₂ClFS₆Hed_{13.2}Jd₁₄ClCor_{0.8}).

Table 1: Bulk composition models (wt.%), phase composition (mol%) and physical properties of garnet harzburgite (Hzb), garnet lherzolite (Lh), average garnet peridotite (GP) and primitive mantle (PM) composition in the NaTiCFMAS system^a.



taken from the PREM model. Chemical reactions in this system are independent of oxygen fugacity. Addition of Al₂O₃, Na₂O and TiO₂ is important for stability of garnet, clinopyroxene and ilmenite (Table 1).

Input data for the thermodynamic quantities are summarized in the THERMOSEISM database. The database was established by supplementing the calorimetric data for low-pressure phases and the EOS for low- and high-pressure phases with the data calculated from the high-*P-T* experiments [11,36]. The output *P-T* results contain the self-consistent information on phase assemblage (the mineral phases, their proportions and individual chemical compositions), the total density and seismic velocities. The aggregate elastic properties were estimated by Voigt-Reuss-Hill averaging. The effect of uncertainties in the computation procedure (phase composition and physical properties) depends on the thermodynamic database used [21-27,36,37]. The uncertainties in the input thermodynamic quantities are common for all compositions and are less significant than those in the seismic models.

Discrepancies in the calculations can be associated with different input parameters such as key values, EOS and form of presentation of EOS, interaction parameters, etc. Solution gives the temperature profile in accordance with the seismic velocity and equilibrium phase composition of mineral assemblage and the constraints imposed onto the bulk system composition.

Table 1 presents some model compositions of the Siberian mantle. We are aware that petrological data obtained on xenoliths from a small number of kimberlite pipes may not be representative of the mantle beneath the whole Siberian craton. Here we restrict our analysis to some of xenoliths [19] and use the average composition of garnet peridotite (hereafter GP model) [38]. The asthenospheric mantle is assumed to be composed of the fertile material of the primitive mantle (PM model) close to a pyrolite model [38]. This model is able to satisfy a large range of petrological and geophysical data within the uncertainties of seismic models and mineral physics data [1,9].

We consider four petrological models, which span a large range of Al₂O₃ (0.4-4.5%), CaO (0.2-3.6%) and FeO/MgO concentrations (Table 1): (1) a strongly depleted garnet harzburgite, (2) a somewhat depleted garnet lherzolite, (3) GP model, (4) PM model. These compositions may help quantitatively interpret seismic models. Other mantle rocks such as amphibole or carbonate-bearing assemblages are unlikely to determine velocities averaged over ~3000 km length scales. Phase compositions, composition of coexisting phases and physical properties are shown in Table 1. Cratonic mantle temperatures and densities are calculated (unless noted otherwise) for depleted compositions at depths of 100-180 km and for fertile PM composition at greater depths. Our results indicate an upper mantle mineralogy as consisting chiefly of olivine, two aluminous pyroxenes and garnet down to about 300 km depth, where the two pyroxenes are replaced by a single high-pressure Cpx. This phase transition is not modeled in the present study.

An evaluation of uncertainties has shown that seismic velocities can provide temperature estimates within ±100°C. For a given chemical composition, the effect of temperature variations of ±100°C causes less than ±0.015 g cm⁻³ (±0.4%) density variations and ±0.04 km s⁻¹ (±0.5%) P-velocity variations. The effect of pressure variations of ±1 GPa (±30 km) causes less than ±0.025 g cm⁻³ (±0.7%) density variations and ±0.08 km s⁻¹ (±1%) P-velocity variations, that is less or close to estimated uncertainties in observed P-velocities [17]. Thus, uncertainties in thermodynamic parameters and in observed velocities do not allow us to constrain temperatures and thickness of the thermal boundary layer from seismic models any tighter than ±100°C and ±30 km.

In addition, we examined the influence on the velocity and density of changing the composition (Table 1, Figures 4a and b). We find that P-velocities for the fertile (basalt rich) primitive mantle composition are slightly greater (≤0.3%) than those for the depleted rocks (Figure 4a). These differences are within the uncertainty and can be explained by the thermodynamic model used. The GP composition has low density relative to PM (Figure 4b) but similar seismic velocities (Figure 4a). Interestingly, the velocities of xenoliths from the Udachnaya pipe are located near the conductive geotherm of 40 mW m⁻² (Figure 4a), while their density are near the conductive geotherm 35 mW m⁻² (Figure 4b).

Compositional gradients from depleted to fertile material lead to a significant change in density ($\Delta\rho/\rho \sim 2-3\%$, Table 1), resulting in only minor changes in velocities (Figures 4a and b). Change in density by 2% is equivalent to the change in temperature by 500°C. A comparison of densities calculated for granular and sheared garnet peridotites from the Udachnaya pipe with the AK135 model density shows that

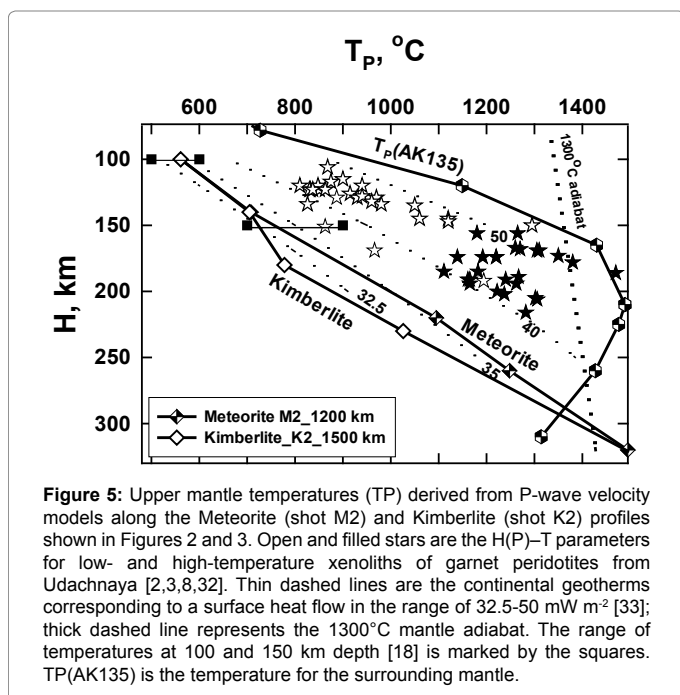


Figure 5: Upper mantle temperatures (T_p) derived from P-wave velocity models along the Meteorite (shot M2) and Kimberlite (shot K2) profiles shown in Figures 2 and 3. Open and filled stars are the $H(P)$ - T parameters for low- and high-temperature xenoliths of garnet peridotites from Udachnaya [2,3,8,32]. Thin dashed lines are the continental geotherms corresponding to a surface heat flow in the range of 32.5-50 mW m^{-2} [33]; thick dashed line represents the 1300°C mantle adiabat. The range of temperatures at 100 and 150 km depth [18] is marked by the squares. $T_p(\text{AK135})$ is the temperature for the surrounding mantle.

“seismic” density is more than 2% denser than that of garnet peridotites (Figure 4b). In the estimates of the P - T points from thermobarometry of garnets no corrections have been made for the effect of Cr owing to the lack of adequate data. The effect of water and partial melt on seismic velocities of cold cratonic mantle is not considered here. We ignore also the effect of grain size on an elasticity due to the lack of experimental data on multi-component solid solutions.

On the whole, the compositional changes from depleted material to fertile primitive mantle have an insignificant impact on the seismic velocities that is practically unresolved by seismic methods [12,20,39], although they are accompanied by noticeable changes in the rock’s density (Figures 4a and b) temperature is the main parameter affecting seismic velocities. Therefore, seismic velocities can be used to directly invert for mantle temperatures. A correct thermal interpretation must account for the dissipative effects due to anelasticity; this procedure is described in [20,21,25]. The uncertainty resulting from the anelastic correction is negligible in the cold cratonic mantle. However, anelasticity can have an important effect on seismic properties, particularly when temperatures approach the solidus in the deeper mantle.

Results and Discussion

Fertility can increase gradually or in a step-wise manner with depth. As noted above (Figure 4), the effect of composition on the seismic velocities and consequently the estimated temperature plays a relatively minor role and is within the uncertainty involved in the thermodynamic calculations and seismic observations [20]. For simplicity, we approximate here a multi-layer structure of cratonic mantle [7] by the depleted GP composition at depths of 100-180 km and by the fertile PM composition at greater depths. We converted to temperature and density the P-wave velocity models shown in Figure 2 together with these compositional models. Average temperature profile for the surrounding mantle ($T_p(\text{AK135})$), which is approximated by the PM composition is inferred from the AK135 model [29]. Because this model shows low wave speeds compared to regional seismic models (Figure 3), the temperature derived for the surrounding mantle is much higher than that of the regional models.

Uncertainties in the derived temperatures result from a number of sources, including uncertainty in the mantle composition and thermoelastic and anelastic properties of minerals. Basic limitations imposed by the seismic data are due to the small number of PNEs, covering a small area of the region (Figure 1). The present-day thermal regime of cratonic mantle is compared with $H(P)$ - T parameters of garnet peridotite xenoliths from the Mir, Udachnaya and Obnazhennaya pipes (Figure 5). The thickness of the thermal boundary layer (TBL), containing a conductive lid and a transition layer, is defined by the depth of the intersection of a cratonic geotherm with the mantle 1300°C adiabat, which is thought to be a reasonable estimate of temperature of the asthenosphere [9,40].

Temperature profiles

A conversion of mantle P-velocities along the cross-cutting Meteorite and Kimberlite profiles for the shot points M2 and K2 situated in the neighborhood and close to the craton’s center (Figure 1) reveals similar temperatures (Figure 5) at depths between 100 km ($T_p \sim 560^\circ\text{C}$) and 140 km ($T_p \sim 700^\circ\text{C}$) in accord with surface heat-flow data [18]. The average values of the thermal gradient (3.5-4.7°C km^{-1}) are 1.5 times lower than the paleotemperature gradients for ancient cratons [6]. The T_p profiles lie below the $H(P)$ - T estimates for the low- and high-temperature garnet peridotites from Yakutian kimberlite pipes and substantially lower than $T_p(\text{AK135})$. The present-day seismic geotherms pass close to the 32.5-35 mW m^{-2} conductive models and intersect the mantle adiabat at ca. 300 km depth and $\sim 1450^\circ\text{C}$ (Figure 5). From garnet thermobarometry [7] and from shear wave seismic tomography [33] the temperatures beneath the SC are also estimated to be close to the 35 mW m^{-2} geotherm (Figure 5). Temperatures inferred from the AK135 model for the surrounding mantle are ~ 300 - 400°C higher than temperatures beneath the ancient Siberian craton (Figure 5). The AK135 model producing maximal temperatures at ~ 220 km reveal inflection with a negative gradient at depths below ~ 220 km, leading to non-physical behavior of the temperature. This can be explained by the fact that at depths between 210 and 300 km the seismic gradient in the AK135 model is two times greater than the P -velocity gradient ($\Delta V_p/\Delta H \sim 0.0017 \text{ s}^{-1}$) in the regional models. This rapid growth in the global velocity model leads to a decrease in temperature with depth. It has been pointed out the difficulties for interpreting the reference models in terms of temperature and composition [11,25,27].

2-D temperature models are shown in Figure 6. On average, there is a systematic decrease in temperature from west to east for the Kimberlite profile (Figure 6a) and a weak decrease from NW to SE for the Meteorite profile (Figure 6b). Lateral temperatures within the root vary appreciably at depths up to ca. 200 km reflecting somewhat different thermal state along the cross-cutting profiles. At greater depths, lateral changes in temperatures carry an insignificant effect implying

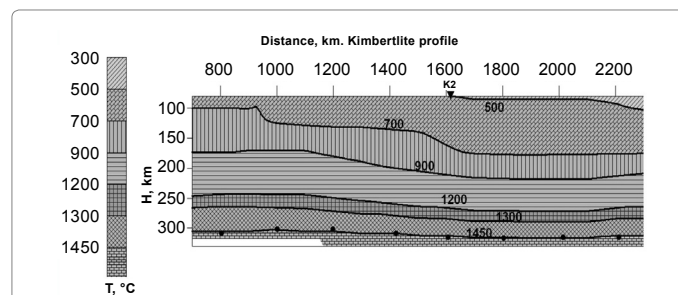


Figure 6a: 2-D temperature models in the mantle beneath the Siberian craton along the cross-cutting profiles Kimberlite and Meteorite

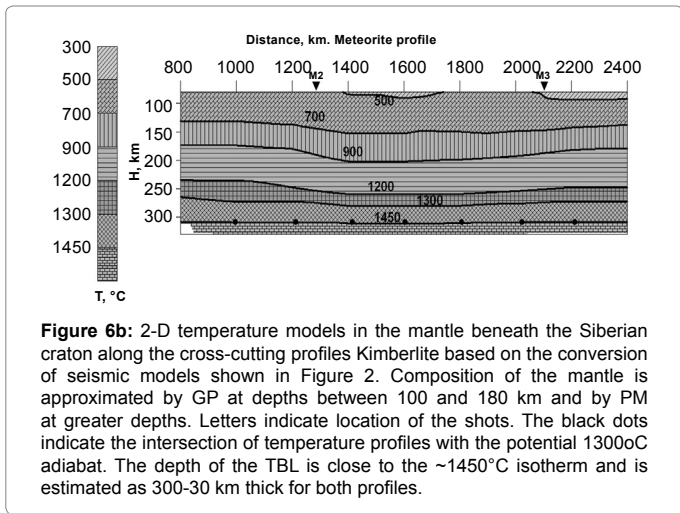


Figure 6b: 2-D temperature models in the mantle beneath the Siberian craton along the cross-cutting profiles Kimberlite based on the conversion of seismic models shown in Figure 2. Composition of the mantle is approximated by GP at depths between 100 and 180 km and by PM at greater depths. Letters indicate location of the shots. The black dots indicate the intersection of temperature profiles with the potential 1300oC adiabat. The depth of the TBL is close to the ~1450°C isotherm and is estimated as 300-30 km thick for both profiles.

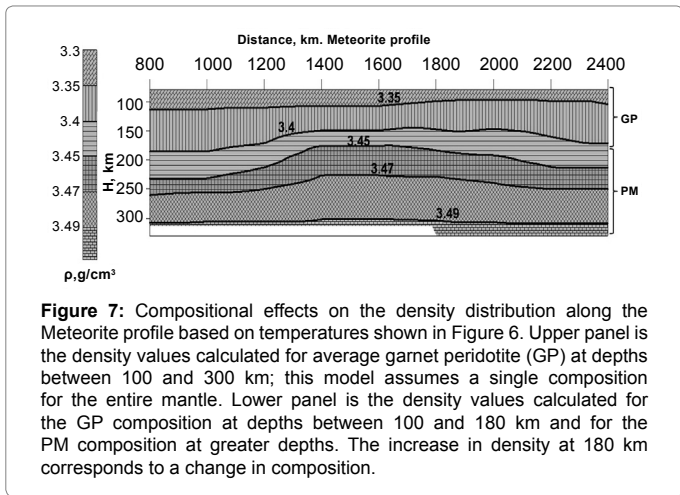


Figure 7: Compositional effects on the density distribution along the Meteorite profile based on temperatures shown in Figure 6. Upper panel is the density values calculated for average garnet peridotite (GP) at depths between 100 and 300 km; this model assumes a single composition for the entire mantle. Lower panel is the density values calculated for the GP composition at depths between 100 and 180 km and for the PM composition at greater depths. The increase in density at 180 km corresponds to a change in composition.

that the inferred thermal heterogeneity diminishes rapidly below 200 km depth. At a depth ca. 300 km, the derived temperatures provide similar estimates. Within the uncertainty of the analysis the craton’s center is somewhat colder than its marginal parts. The temperature profiles exhibit a substantial decrease in temperature beneath the SC as compared to the average temperature in the surrounding mantle. For example, the 900°C isotherm under the SC lies at depths of 170-200 km (Figure 6), while according to the AK135 model, this temperature corresponds to a depth of ~90 km (Figures 5, 6a and 6b).

Density profiles

2-D Kimberlite and Meteorite velocity models (Figure 2) were converted to the 2-D density profiles (Figures 7 and 8) based on temperatures shown in Figure 6. Note that lateral density variations in Figures 7 and 8 are due to thermal rather than compositional anomalies; the increase in density at a depth of 180 km corresponds to a change in the composition from GP to PM (Figure 8a and b).

Figure 7 (upper panel) demonstrates that the density of the depleted GP composition at the base of the TBL ($\rho(310 \text{ km}, 1450^\circ\text{C}) \sim 3.42 \text{ g cm}^{-3}$) is 2% less dense than the AK135/PREM model density at the same depth. This means that the density of the depleted cratonic mantle would be globally reduced up to 300 km, which is apparently not the case in reality. Such a composition seems to be too buoyant to represent the composition of the entire cratonic mantle [2,3], as well as to satisfy

the density of the surrounding mantle [28] and the isopycnic hypothesis (i.e., compensation of thermal and compositional effects) [1]. On the other hand, Figure 7 (lower panel) shows that the density of the fertile PM composition at the base of the TBL ($\rho(310 \text{ km}, 1450^\circ\text{C}) \sim 3.49 \text{ g cm}^{-3}$) is consistent with the PREM model density. This density contrast of 2% is equivalent to temperature contrast of ~500°C. If cratonic mantle would have had a depleted composition with a density of 3.49 g cm^{-3} , the temperature at the base of the TBL would be ~950°C. Such a cold mantle does not correspond to either thermal models [15,18] or thermobarometry estimates for peridotite xenoliths [7,8]. Moreover, a temperature contrast of 500°C must lead to a significant increase in P-velocity ($V_p(\text{GP}, 310 \text{ km}/950^\circ\text{C}) \sim 8.73 \text{ km s}^{-1}$) that is not observed in global and regional seismic models, according to which $V_p(310 \text{ km}) \sim 8.5\text{-}8.6 \text{ km s}^{-1}$ (Figures 2 and 3).

Thickness of the thermal boundary layer

Temperatures of the cratonic mantle are much lower than the average temperature for the surrounding mantle and pass near the conductive geotherms of 32.5-35.0 mW m^{-2} (Figure 5), that leads to an increase in the thickness of the mantle beneath the Siberian craton up to ca. 300 km. Figure 6 shows that the depth of the TBL is close to the 1450 100°C isotherm and is estimated about $300 \pm 30 \text{ km}$ thick for both profiles. These results are consistent with the values of the root thickness estimated from heat flow observations, thermobarometry and tomographic models [7,18,41]. It has been found [7] that the Yakutsk kimberlite field has temperatures that are close to a 35 mW m^{-2} geotherm, which intersects the mantle adiabat at ca. 300 km depth. A similar conclusion may be inferred from [33], where the inversion of seismotomographic data gives the 32.5-35 mW m^{-2} conductive geotherms over most of the central Archean parts of the SC. This means

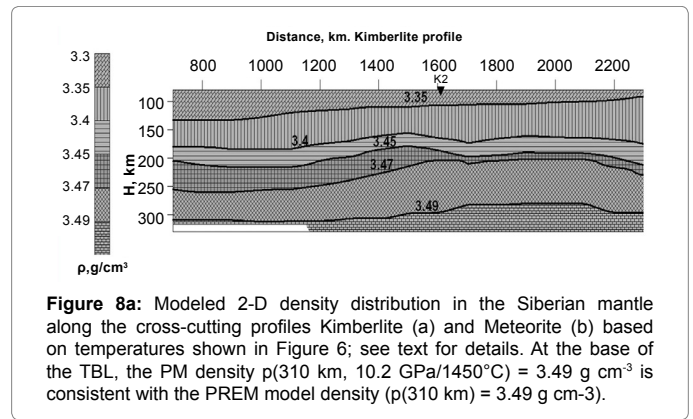


Figure 8a: Modeled 2-D density distribution in the Siberian mantle along the cross-cutting profiles Kimberlite (a) and Meteorite (b) based on temperatures shown in Figure 6; see text for details. At the base of the TBL, the PM density $\rho(310 \text{ km}, 10.2 \text{ GPa}/1450^\circ\text{C}) = 3.49 \text{ g cm}^{-3}$ is consistent with the PREM model density ($\rho(310 \text{ km}) = 3.49 \text{ g cm}^{-3}$).

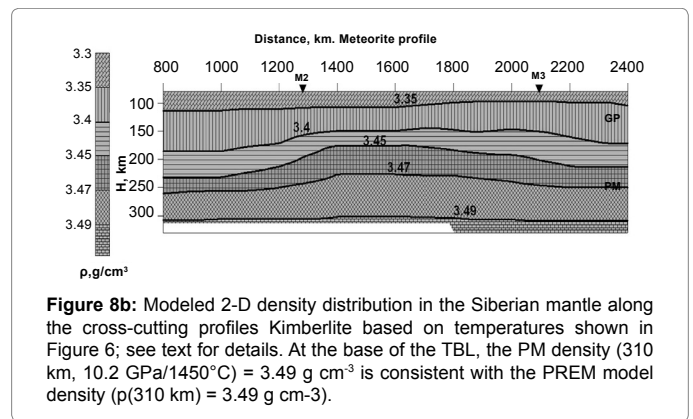


Figure 8b: Modeled 2-D density distribution in the Siberian mantle along the cross-cutting profiles Kimberlite based on temperatures shown in Figure 6; see text for details. At the base of the TBL, the PM density $\rho(310 \text{ km}, 10.2 \text{ GPa}/1450^\circ\text{C}) = 3.49 \text{ g cm}^{-3}$ is consistent with the PREM model density ($\rho(310 \text{ km}) = 3.49 \text{ g cm}^{-3}$).

that, although the approaches and methods are different, the results are mutually consistent.

For the Yakutsk kimberlite province, the heat flow values are estimated at the level of 20-30 mW m⁻² [15], which indicate that temperatures under this part of the craton are the lowest among Precambrian provinces. The present-day thermal regime of the cratonic mantle can be estimated from the temperature slopes shown in Figure 5. With an average *T* gradient of 3.5 K km⁻¹ and an average thermal conductivity of 3-4 W m⁻¹ K⁻¹ [18], we obtain the upper mantle heat flow value of 10-14 mW m⁻². For major Precambrian provinces, the typical estimates of mantle heat flow based on various assumptions are within the range 11-20 mW m⁻² [18,24].

Increase in fertility at a depth of ~180 km corresponding to the proposed change in the composition is accompanied by an increase in density. Comparison with the AK135/PREM models shows that the depleted compositions are less dense while the fertile PM composition is denser than the "seismic" density at least at 100-200 km (Figures 4b, 7 and 8). At these depths, the Siberian mantle has lower temperatures, higher velocities, and lower densities than the surrounding mantle. The basic conclusion arising from our calculations is that the results seem unable to explain a reasonable density distribution for any uniform composition (either depleted or fertile) throughout the entire cratonic mantle. Thus, the cratonic mantle is chemically stratified and becomes more fertile in composition with depth.

Figures 7 and 8 illustrate pronounced variations in density both lateral and vertical and show that the PM density at the base of cratonic mantle (~300 km) is consistent with the average density of the ambient mantle according to the PREM model at the same depth (Figure 4b). Geotherms calculated from absolute velocities for various petrological models (Hzb, Lh, GP, PM) differ from each other by less than 50°C [20] due to a minor influence of the composition on the seismic velocities (Figure 4a). This means that discrimination of fine differences in the composition of the cratonic mantle by seismic methods only does not seem possible. Jones et al. [39] based on mineral physics data found that a contrast between a harzburgitic and lherzolitic mantle should not be detectable seismically, and only marginally in conductivity. This implies that the thickness of the cratonic mantle does not depend significantly on the composition.

All density and temperature profiles are fairly similar at about 300 km (Figures 6 and 8), assuming that at this depth the mantle under Siberia is not appreciably distinct from the underlying asthenosphere. However as noted in [34], the refertilised zone may still constitute an intact lithospheric root, cooler and somewhat less fertile than the surrounding mantle. The more fertile material at the base of the root, where the lithosphere and the asthenosphere have about the same temperature, must not differ strongly in physical and chemical characteristics from that of adjacent convecting mantle. Our analysis shows that the density variations in the lower part of the root due to the chemical composition are greater than those caused by temperature (Figures 6-8). Such a cratonic keel model reconciles petrological and geophysical evidence and is in qualitative agreement with other studies [12,35,42,43]. However interpretation of the multi-layer structure of the mantle keel remains somewhat speculative, because conclusions about the fine details of the thermo-chemical structure of the Siberian mantle are difficult to deduce only from seismic observations. A more thorough analysis requires additional data on seismic, gravity, heat-flow and magnetotelluric observations.

Conclusions

1. Using a thermodynamic-geophysical approach and petrologically-based constraints, we map the 2-D interior structure of the Siberian cratonic mantle along the cross-cutting seismic profiles Kimberlite and Meteorite. Cratonic mantle shows significant heterogeneity in the distribution of seismic velocities, temperature and density, the relief of seismic boundaries and the degree of layering at depths up to ~200 km reflecting somewhat different thermal state along both seismic profiles. At greater depths, the lateral changes in the thermal state and physical properties are minor. Temperatures of the cratonic mantle derived from the Kimberlite and Meteorite profiles pass near the 32.5-35 mW m⁻² conductive models, below the *H(P)*-*T* estimates for the low- and high-temperature garnet peridotites from Yakutian kimberlite pipes and significantly lower than the average temperature for the surrounding mantle.
2. A change of composition from depleted to fertile material reveals a negligible effect on seismic velocities that is practically unresolved by seismic methods, but remains the most important factor for the density increase of cratonic root. The more fertile material at the base of the root, where the lithosphere and the asthenosphere have about the same temperature, must not differ strongly in physical and chemical characteristics from that of adjacent convecting mantle.
3. The distribution of density in the Siberian mantle cannot be attributed to any single composition, either depleted or enriched in basaltic components. The density heterogeneities should be related not only to thermal anomalies, but also to changes in chemical composition with depth. Effect of compositional changes (from garnet peridotite to primitive mantle material) on the density-depth structure is more important than the effect of thermal variations. This conclusion suggests significant fertilization at depths greater than ~180 km and is compatible with chemical stratification in the craton root.
4. Within the model resolution, the thickness of the thermal boundary layer (conductive lid + transition layer) can be estimated as 300 ± 30 km thick along the Kimberlite and Meteorite profiles; temperature at the base of the TBL is close to the 1450 ± 100°C isotherm. At the base of the TBL, the calculated density is consistent with the PREM model density. We find that both compositional and thermal anomalies are required to explain the mantle internal structure along both seismic profiles by a keel model consisting of depleted garnet peridotite at depths of 100 to 180 km and more fertile material at greater depths.

Acknowledgment

This research was supported by Russian Academy of Sciences under Programs 22 and 28 and by RFBR grant 12-05-00033.

References

1. Jordan TH (1978) Composition and development of the continental tectosphere. *Nature* 274: 544-548.
2. Solovyeva LV, Vladimirov BM, Dneprovskaya LV (1994) Kimberlites and kimberlite-like rocks. Upper mantle beneath ancient platforms. Nauka, Novosibirsk (in Russian).
3. Boyd FR, Pokhilenko NP, Pearson DG, Mertzman SA, Sobolev NV, et al, (1997) Composition of the Siberian cratonic mantle: evidence from Udachnaya peridotite xenoliths. *Contrib Mineral Petrol* 128: 228-246.
4. Rosen OM, Manakov AV, Zinchuk NN (2006) The Siberian Craton: Formation, Diamond Content. Nauchnyi Mir, Moscow (in Russian).

5. Pearson DG, Wittig N, (2008) Formation of Archaean continental lithosphere and its diamonds: the root of the problem. *J Geol Soc* 165: 895-914.
6. Glebovitsky VA, Nikitina LP, Khil'tova VYa (2001) The thermal state of the mantle underlying precambrian and phanerozoic structures: Evidence from garnet-orthopyroxene thermobarometry of garnet peridotite xenoliths in kimberlites and alkali basalts. *Izv Phys Solid Earth* 37: 193-214.
7. Ashchepkov IV, Pokhilenko NP, Vladykin NV, Logvinova AM, Afanasiev VP et al, (2010) Structure and evolution of the lithospheric mantle beneath Siberian craton, thermobarometric study. *Tectonophysics* 485: 17-41.
8. Ionov DA, Doucet LS, Ashchepkov IV (2010) Composition of the lithospheric mantle in the Siberian Craton: new constraints from fresh peridotites in the Udachnaya-East kimberlite. *J Petrol* 51: 2177-2210.
9. Poudjom Djomani YH, O'Reilly SY, Griffin WL, Morgan P (2001) The density structure of sub continental lithosphere through time. *Earth Planet Sci Lett* 184: 605-621.
10. Kuskov OL, Kronrod VA (2007) Composition, temperature, and thickness of the lithosphere beneath the Archean Kaapvaal craton. *Izv Phys Solid Earth* 43: 42-62.
11. Kuskov OL, Kronrod VA, Annersten H (2006) Inferring upper-mantle temperatures from seismic and geochemical constraints: Implications for Kaapvaal craton. *Earth Planet Sci Lett* 244: 133-154.
12. Afonso JC, Fernandez M, Ranalli G, Griffin WL, Connolly JAD (2008) Integrated geophysical-petrological modelling of the lithospheric-sublithospheric upper mantle: methodology and applications. *Geochem Geophys Geosyst*.
13. Egorkin AV (2004) Mantle structure of the Siberian platform. *Izv Phys Solid Earth* 35: 385-394.
14. Fuchs K (Ed) (1997) Upper Mantle Heterogeneities from Active and Passive Seismology. NATO ASI series. Kluwer Academic Publishers, Dordrecht-Boston-London 17.
15. Duchkov AD, Sokolova LS (1997) The thermal structure of the lithosphere beneath the Siberian platform. *Rus Geol Geophys* 38: 494-503.
16. Thybo H (2006) The heterogeneous upper mantle low velocity zone. *Tectonophysics* 416: 53-79.
17. Pavlenkova GA, Pavlenkova NI (2006) Upper mantle structure of the Northern Eurasia from peaceful nuclear explosion data. *Tectonophysics* 416: 33-52.
18. Artemieva IM, Mooney WD (2001) Thermal thickness and evolution of Precambrian lithosphere: A global study. *J Geophys Res* 106: 16387-16414.
19. Griffin WL, O'Reilly SY, Abe N, Aulbach S, Davies RM et al (2003) The origin and evolution of Archean lithospheric mantle. *Precambrian Res* 127: 19-41.
20. Kuskov OL, Kronrod VA, Prokof'ev AA (2011) Thermal structure and thickness of the lithospheric mantle underlying the Siberian Craton from the Kraton and Kimberlit superlong seismic profiles. *Izv Phys Solid Earth* 47: 155-175.
21. Sobolev SV, Zeyen H, Stoll G, Werling F, Altherr R, et al, (1996) Upper mantle temperatures from teleseismic tomography of French Massif Central including effects of composition, mineral reactions, anharmonicity, anelasticity and partial melt. *Earth Planet Sci Lett* 139: 147-163.
22. Shapiro NM, Ritzwoller MH (2004) Thermodynamic constraints on seismic inversions. *Geophys J Int* 157: 1175-1188.
23. Kronrod VA, Kuskov OL (2006) Determining heat flows and radiogenic heat generation in the crust and lithosphere based on seismic data and surface heat flows. *Geochem International* 44: 1035-1040.
24. Kronrod VA, Kuskov OL (2007) Modeling of the thermal structure of continental lithosphere. *Izv Phys Solid Earth* 43: 91-101.
25. Cammarano F, Romanowicz B, Stixrude L, Lithgow-Bertelloni C, Xu W (2009) Inferring the thermochemical structure of the upper mantle from seismic data. *Geophys J Int* 179: 1169-1185.
26. Khan A, Zunino A, Deschamps F (2013) Upper mantle compositional variations and discontinuity / topography imaged beneath Australia from Bayesian inversion of surface-wave phase velocities and thermochemical modeling. *J Geophys Res* 118: 5285-5306.
27. Tumanian M, Frezzotti ML, Peccerillo A, Brandmayr E, Giuliano F, Panza GF (2012) Thermal structure of the shallow upper mantle beneath Italy and neighbouring areas: Correlation with magmatic activity and geodynamic significance. *Earth-Sci Rev* 114: 369-385.
28. Dziewonski AM, Anderson DL (1981) Preliminary reference Earth model. *Phys Earth Planet Inter* 25: 297-356.
29. Kennett BLN, Engdahl ER, Buland R (1995) Constraints on seismic velocities in the Earth from travel times. *Geophys J Int* 122: 108-124.
30. Pavlenkova NI (1982) The intercept-time method: possibilities and limitations. *J Geophysics* 51: 85-95.
31. Pavlenkova NI (2011) Seismic structure of the upper mantle along the long-range PNE profiles rheological implication. *Tectonophysics* 508: 85-95.
32. Shimizu N, Pokhilenko NP, Boyd FR, Pearson DG (1997) Geochemical characteristics of mantle xenoliths from Udachnaya kimberlite pipe. *Russ Geol Geophys* 38: 194-205.
33. Deen TJ, Griffin WL, Begg G, O'Reilly SY, Natapov LM, et al, (2006) Thermal and compositional structure of the subcontinental lithospheric mantle: Derivation from shear wave seismic tomography. *Geochem Geophys Geosyst*.
34. O'Reilly SY, Griffin WL (2010) The continental lithosphere-aesthenosphere boundary: Can we sample it? *Lithos* 120: 1-13.
35. Arndt NT, Coltice N, Helmstaedt H, Gregoire M (2009) Origin of Archean subcontinental lithospheric mantle: Some petrological constraints. *Lithos* 109: 61-71.
36. Kuskov OL (1997) Constitution of the Moon: 4. Composition of the mantle from seismic data. *Phys Earth Planet Inter* 102: 239-257.
37. Stixrude L, Lithgow-Bertelloni C (2011) Thermodynamics of mantle minerals – II. Phase equilibria. *Geophys J Int* 184: 1180-1213.
38. McDonough WF (1990) Constraints on the composition of the continental lithospheric mantle. *Earth Planet Sci Lett* 101: 1-18.
39. Jones AG, Evans RL, Eaton DW (2009) Velocity-conductivity relationships for mantle mineral assemblages in Archean cratonic lithosphere based on a review of laboratory data and Hashin Shtrikman extremal bounds. *Lithos* 109: 131-143.
40. Eaton DW, Darbyshire F, Evans RL, Grütter H, Jones AG, Yuan X (2009). The elusive lithosphere-aesthenosphere boundary (LAB) beneath cratons. *Lithos* 109: 1-22.
41. Bushenkova N, Tychkov S, Koulakov I (2002) Tomography on PP-P waves and its application for investigation of the upper mantle in central Siberia. *Tectonophysics* 358: 57-76.
42. King SD (2005) Archean cratons and mantle dynamics. *Earth Planet Sci Lett* 234: 1-14.
43. Stepashko AA (2013) The structure of the lithospheric mantle of the Siberian craton and seismodynamics of deformation waves in the Baikal seismic zone. *Geodynamics & Tectonophysics* 4: 387-415.